

# Numerical and experimental study of aerodynamic noise by a small wind turbine



Seunghoon Lee<sup>a,\*</sup>, Soogab Lee<sup>b</sup>

<sup>a</sup>Department of Mechanical and Aerospace Engineering, Seoul National University, Seoul 151-744, Republic of Korea

<sup>b</sup>Center for Environmental Noise and Vibration Research, Engineering Research Institute, Seoul National University, Seoul 151-744, Republic of Korea

## ARTICLE INFO

### Article history:

Received 5 February 2013

Accepted 15 July 2013

Available online 13 August 2013

### Keywords:

Small wind turbine

Semi-empirical model

Airfoil self-noise

Turbulence ingestion noise

Noise measurement

## ABSTRACT

To examine the aerodynamic noise produced by small wind turbines, this study predicts and measures the aerodynamic noise from a 10 kW wind turbine. The numerical predictions include the turbulence ingestion noise, turbulent-boundary-layer trailing edge noise, and trailing edge bluntness noise. The noise measurement is carried out with free-field microphones at a reference position according to the IEC 61400-11 standard. Although the trailing edge bluntness noise is under-predicted at low wind speeds, the spectral trends of the prediction results generally agree well with those of the experimental data. It is also found that for small wind turbines, the trailing edge bluntness noise can be an important noise source.

Crown Copyright © 2013 Published by Elsevier Ltd. All rights reserved.

## 1. Introduction

Wind turbines transform wind energy into electric energy without producing any waste. However, they make noise due to the rotational motion of the wind turbine blades. This noise can exert a negative influence on people near wind turbines. Accordingly, it is important to evaluate the noise generated from wind turbines.

Several previous studies have numerically and experimentally examined the noise produced by wind turbines. Zhu et al. modeled the aerodynamic noise from a 300 kW wind turbine using a semi-empirical model, and they compared the predicted results with measurement data [1]. Although the semi-empirical model that they used was in terms of NACA0012 airfoil, they successfully calculated the wind turbine noise by altering the input data of the boundary layer displacement thickness so that it matched the data pertaining to the actual airfoil shape of the wind turbine blade. Oerlemans and Schepers predicted the noise from two large wind turbines using the same empirical model [2]. They measured the wind turbine noise using a microphone array and then validated the prediction results with experimental data. These previous studies found that the main source of wind turbine noise is the

aerodynamic noise from the wind turbine blades, also showing that this noise has a broadband spectrum.

However, while many studies have focused on the noise from large wind turbines, noise from small wind turbines has not been thoroughly investigated thus far. The Reynolds number of the flow around small wind turbine blades is generally smaller than that around large wind turbine blades. Due to this difference, the aerodynamic noise made by small wind turbines can differ from that of large wind turbines. In addition, small wind turbines are typically installed close to residences compared to large wind turbines. As a result, people can be more annoyed by the noise from a small wind turbine as compared to a more distant large wind turbine. Thus, it is necessary to examine the aerodynamic noise from small wind turbines.

The purpose of this study is to evaluate the aerodynamic noise generated from a small wind turbine. Based on a 10 kW small wind turbine, the aerodynamic noise is predicted using empirical models proposed by Lowson [3] and Brooks et al. [4]. Noise measurements are also carried out to validate the results of the numerical predictions. Using these results, we assess the noise characteristics of the small wind turbine.

## 2. Numerical method

The aerodynamic noise that is generated from wind turbine blades is composed of turbulence ingestion noise and airfoil self-noise [3]. The turbulence ingestion noise occurs when

\* Corresponding author. Rm. 105, Bldg. 311, Department of Mechanical and Aerospace Engineering, Seoul National University, Daehak-dong, Gwanak-gu, Seoul 151-744, Republic of Korea. Tel.: +82 2 880 7384; fax: +82 2 876 4360.

E-mail address: [kami00@snu.ac.kr](mailto:kami00@snu.ac.kr) (S. Lee).

**Nomenclature***Latin letters*

$C$	chord length (m)
$c_0$	speed of sound (m/s)
$\overline{D}_h$	high frequency directivity function
$\overline{D}_l$	low frequency directivity function
$h$	height from the ground (m)
$h_e$	trailing edge thickness (m)
$h_{\min}$	minimum trailing edge height (mm)
$K_{lc}$	low-frequency correction factor
$\hat{k}$	normalized wave number
$l_T$	atmospheric turbulence length scale (m)
$l$	span (m)
$M$	Mach number
$r_e$	distance from source to observer (m)

SPL	sound pressure level (dB)
St	Strouhal number
$\overline{w}$	turbulence intensity
$z$	ground roughness

*Greek letters*

$\delta^*$	boundary layer displacement thickness (m)
$\rho$	air density (kg/m <sup>3</sup> )

*Subscripts*

TEBN	trailing edge bluntness noise
TEN	trailing edge noise
TIN	turbulence ingestion noise
$\alpha$	angle of attack effect
p	pressure side
s	suction side

atmospheric turbulence is ingested into the wind turbine rotor, while the airfoil self-noise is generated regardless of the atmospheric turbulence. The airfoil self-noise is composed of turbulent-boundary-layer trailing edge noise, laminar-boundary-layer vortex shedding noise, trailing edge bluntness noise, and tip noise [4]. Because wind turbines operate in an open environment, the boundary layers on the blades are typically turbulent at the trailing edge. This leads to the generation of turbulent-boundary-layer trailing edge noise. Moreover, trailing edge bluntness noise can be produced by the blades unless the blades have sharp trailing edges. Thus, the turbulence ingestion noise, the turbulent-boundary-layer trailing edge noise, and the trailing edge bluntness noise are modeled by a numerical prediction method.

In addition, because steady loading is applied to the rotating blade as it operates, low-frequency loading noise can be generated from the wind turbine rotor. This loading noise is one of the main noise sources of rotating machinery, such as helicopter rotors, turbo-machinery, and fans. However, for a wind turbine rotor, this low-frequency loading noise is inaudible in most situations, as the rotational speed of a wind turbine is very low. Accordingly, the low frequency loading noise is not calculated in the numerical prediction.

The turbulence ingestion noise is predicted by an empirical model proposed by Lawson [3,5]. According to this model, the frequency spectrum can be expressed as

$$\text{SPL}_{\text{TIN}} = \text{SPL}_{\text{H,TIN}} + 10 \log_{10} \left( \frac{K_{lc}}{1 + K_{lc}} \right), \quad (1)$$

with

$$\text{SPL}_{\text{H,TIN}} = 10 \log_{10} \left\{ \rho^2 c_0^2 l_T \frac{l}{r_e^2} M^3 \overline{D}_l \overline{w}^2 \hat{k}^3 (1 + \hat{k}^2)^{-7/3} \right\} + 58.4, \quad (2)$$

where  $K_{lc}$  is the low-frequency correction factor,  $l_T$  is the atmospheric turbulence length scale,  $\overline{w}$  is the turbulence intensity, and  $\hat{k}$  is the normalized wave number. The atmospheric turbulence length scale and the turbulence intensity are determined from an empirical model using the ground roughness [6]. These are determined as follows:

$$l_T = 25h^{0.35} z^{-0.063} \quad (3)$$

and

$$\overline{w} = \left\{ 0.24 + 0.096 \log_{10} z + 0.016 (\log_{10} z)^2 \right\} \frac{\log(30/z)}{\log(h/z)}, \quad (4)$$

where  $z$  is the ground roughness and  $h$  is the height from the ground.

A semi-empirical model proposed by Brooks et al. is used to calculate the turbulent-boundary-layer trailing edge noise and trailing edge bluntness noise [4]. This model is made based on wind tunnel experiments using a NACA0012 airfoil. With this semi-empirical model, the 1/3 octave band sound pressure levels of the trailing edge noise and trailing edge bluntness noise are calculated as Eqs. (5)–(9).

$$\text{SPL}_{\text{TEN}} = 10 \log \left( 10^{\text{SPL}_{\alpha}/10} + 10^{\text{SPL}_s/10} + 10^{\text{SPL}_p/10} \right), \quad (5)$$

with

$$\text{SPL}_p = 10 \log \left( \frac{\delta_p^* M^5 \overline{D}_h}{r_e^2} \right) + A \left( \frac{\text{St}_p}{\text{St}_1} \right) + (K_1 - 3) + \Delta K_1, \quad (6)$$

$$\text{SPL}_s = 10 \log \left( \frac{\delta_s^* M^5 \overline{D}_h}{r_e^2} \right) + A \left( \frac{\text{St}_s}{\text{St}_1} \right) + (K_1 - 3), \quad (7)$$

$$\text{SPL}_{\alpha} = 10 \log \left( \frac{\delta_{\alpha}^* M^5 \overline{D}_h}{r_e^2} \right) + B \left( \frac{\text{St}_{\alpha}}{\text{St}_2} \right) + K_2, \quad (8)$$

and

$$\begin{aligned} \text{SPL}_{\text{TEBN}} = 10 \log \left( \frac{h_e M^{5.5} \overline{D}_h}{r_e^2} \right) + G_4 \left( \frac{h_e}{\delta_{\text{avg}}^*}, \psi \right) \\ + G_5 \left( \frac{h_e}{\delta_{\text{avg}}^*}, \psi, \frac{\text{St}_{\text{TEBN}}'''}{\text{St}_{\text{peak}}'''} \right). \end{aligned} \quad (9)$$

Detailed descriptions of the functions and the parameters in Eqs. (5)–(9) are explained in the literature [4].

A strip theory approach is used to apply the two-dimensional empirical models to rotating wind turbine blades. Each blade is divided into a number of segments of equal lengths, and the prediction models are then applied to the segments. Moreover, a cardioid-type directivity pattern is used for the prediction of the



Fig. 1. Photograph of the 10 kW small wind turbine.

airfoil self-noise, which is the theoretical directivity for a semi-infinite flat plate. On the other hand, as the frequency range of the turbulence ingestion noise is low, a dipole directivity pattern is applied for the prediction of the turbulence ingestion noise.

### 3. Experiment

The wind turbine model used in this experiment was a 10 kW three-bladed horizontal axis wind turbine which is located in Gyeonggi Province, Korea. Fig. 1 presents a photograph of the wind turbine. The rotor diameter and the hub height of the wind turbine were 8 m and 18 m, respectively. The wind turbine began to rotate at a wind speed of 1.5 m/s, and the rotational speed increased with an increase in the wind speed. The wind turbine reached its rated rotational speed of 180 RPM at a wind speed of about 10 m/s. After a

wind speed of 12 m/s, the wind turbine was stopped by yawing the rotor from the wind direction.

At the test site, a computer was installed and connected to the wind turbine monitoring system. This computer recorded the rotational speed and power output of the wind turbine. Furthermore, an anemometer and a wind vane were mounted on the tower at a height of 10 m from the ground, as shown in Fig. 1. They were used to measure the wind speed and direction at the site during the experiment. These data were also recorded in the computer in 1-min intervals.

Acoustic signals were recorded by three sets of hand-held sound level meters (Brüel & Kjær type 2250) with free-field microphones (Brüel & Kjær type 4190). The microphones were mounted on circular boards 1 m in diameter and were connected to hand-held sound level meters with extension cables. The microphones were covered with foam windscreens to minimize the wind noise. Acoustic signals were recorded with a sampling rate of 48 kHz. One microphone was positioned in the downwind direction at a distance of 22 m from the wind turbine, which is the reference position according to the IEC 61400-11 standard [7]. The other two microphones were placed at an offset of 30° from the downwind position. When the wind turbine yawed more than 15° from the initial position, the other microphone close to the downwind direction took over the acoustic measurement.

The measured acoustic signals were divided into 1-min intervals. The A-weighted sound pressure level was then calculated for each acoustic signal. The 1/3 octave band spectra were also obtained from the acoustic signals. Using these spectra, the average 1/3 octave band spectra were calculated for each integer wind speed bin.

### 4. Results and discussion

The measured power and the rotational speed of the wind turbine with respect to the wind speed are presented in Fig. 2(a) and (b), respectively. Each point shown in Fig. 2 represents data averaged for 1 min. The power began to be generated at a wind speed of about 3 m/s and increased with an increase in the wind speed. During the measurement, the wind speed rose to about 7 m/s. The corresponding rotational speed ranged from about 50 RPM to 170 RPM.

Fig. 3 compares the A-weighted sound pressure levels of the experimental data and the results of the numerical prediction. The prediction results for the three noise sources that comprise the wind turbine aerodynamic noise are also presented in Fig. 3. These results indicate that the turbulence ingestion (TI) noise and the trailing edge bluntness noise were the dominant noise sources of the aerodynamic noise. A previous study suggested that turbulent-

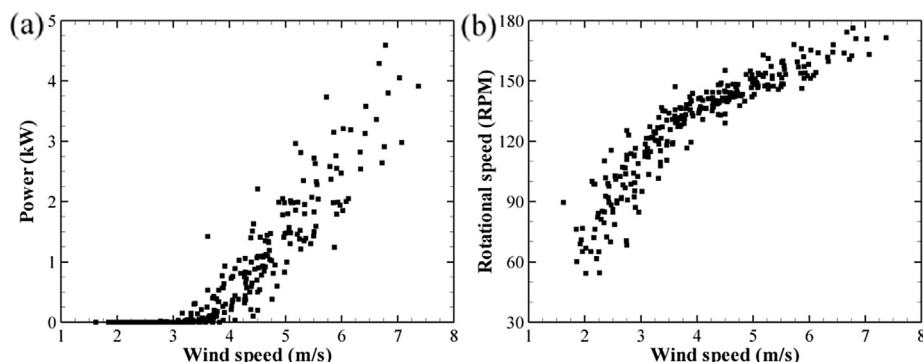


Fig. 2. (a) Measured power and (b) rotational speed with respect to the wind speed.

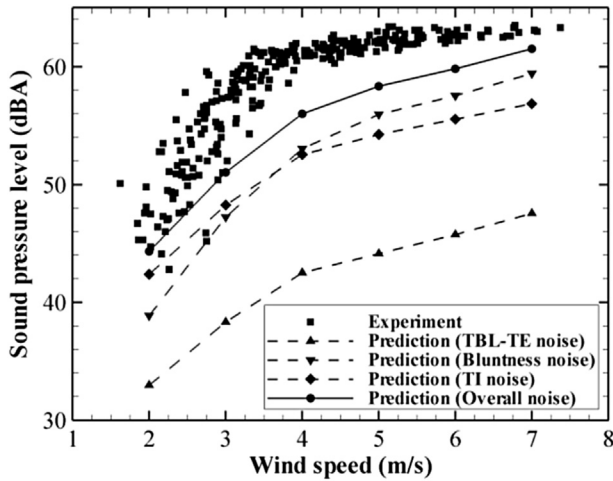


Fig. 3. Comparison between the A-weighted sound pressure levels of the measured data and the numerical prediction results.

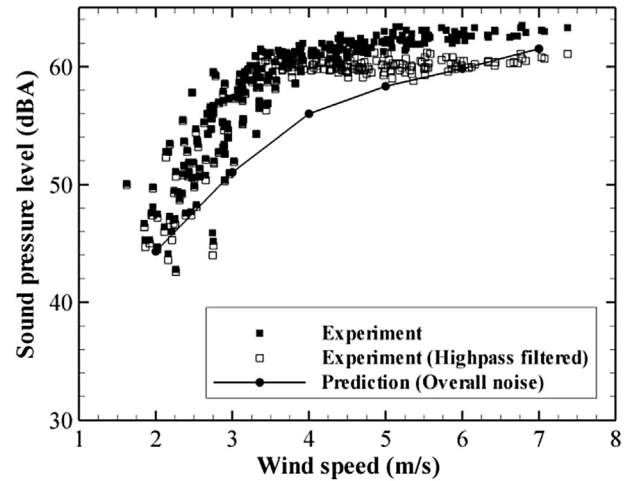


Fig. 5. Comparison between the A-weighted sound pressure levels of the high-pass filtered signals and the numerical prediction results.

boundary-layer trailing edge (TBL-TE) noise is the dominant noise source of large wind turbines [8]. However, in the present case, the turbulent-boundary-layer trailing edge noise had little effect on the overall sound pressure level (OASPL). Moreover, the results show that the numerical results under-predicted the overall sound pressure levels at all wind speeds. The A-weighted sound pressure level from the experimental data was about 3 dB–5 dB higher than that from the numerical predictions.

To examine the discrepancy between the experimental data and the numerical results in more detail, a 1/3 octave band spectrum analysis was performed, as shown in Fig. 4. In the experimental data, a large peak was found from 100 Hz to 200 Hz. This low-

frequency noise is the mechanical noise from the generator. However, this low-frequency mechanical noise cannot be modeled in a numerical analysis because numerical predictions only include the aerodynamic noise from the wind turbine rotor. This is one of the reasons for the underestimated result. In addition, it should be noted that the large peak due to mechanical noise is not a typical characteristic of small wind turbines. The mechanical noise from the 10 kW wind turbine was not reduced well, as it was developed for experimental purposes.

Except for the mechanical noise, the spectral trends of the prediction results agree well with that of the experimental data. The results of the numerical prediction indicate that low-frequency broadband noise was generated due to the turbulent ingestion

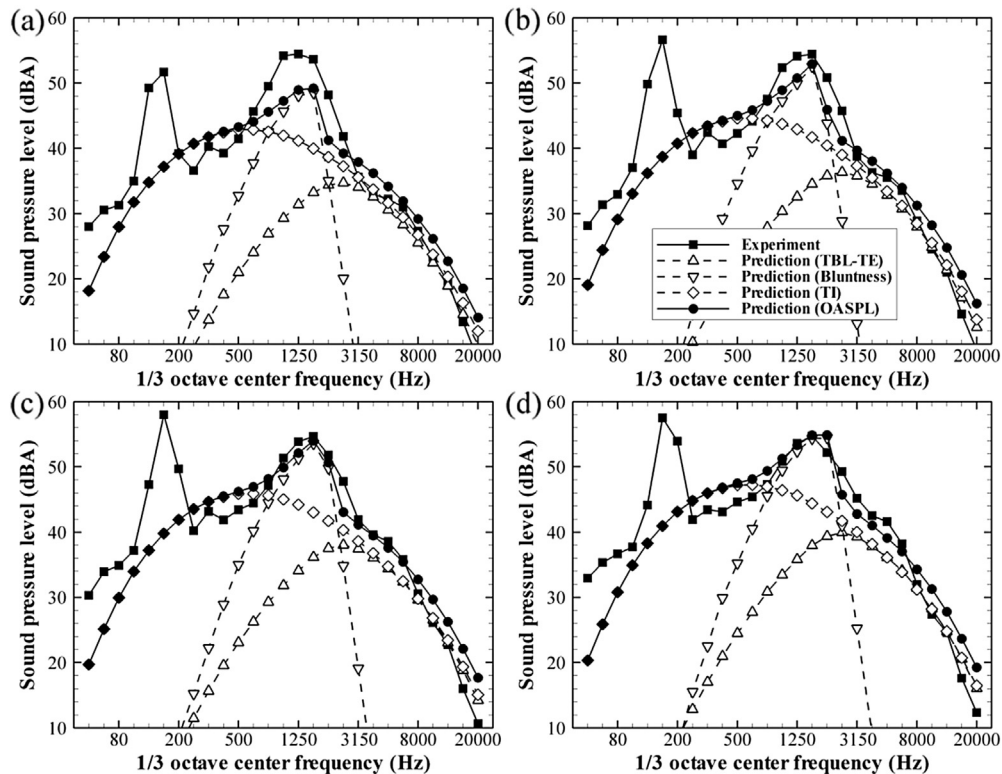


Fig. 4. (a) 1/3 Octave band spectra of the measured data and the numerical predictions at wind speeds of 4 m/s, (b) 5 m/s, (c) 6 m/s, and (d) 7 m/s.

**Table 1**

Normalized boundary layer displacement thickness, the ratio between the trailing edge height and boundary layer displacement thickness, peak frequency, and the minimum trailing edge height at wind speeds from 4 m/s to 7 m/s.

Wind speed (m/s)	$\delta^*/C$	$h_e/\delta^*$	Peak frequency (Hz)	$h_{\min}$ (mm)
4	0.0113	1.41	1270	0.566
5	0.0116	1.38	1390	0.580
6	0.0121	1.32	1480	0.605
7	0.0125	1.28	1580	0.626

noise, while the turbulent-boundary-layer trailing edge noise influenced the high-frequency broadband noise. Furthermore, trailing edge bluntness noise caused a quasi-tone in the frequency range of 1 kHz–2 kHz. However, at low wind speeds, the measured peak level for the trailing edge bluntness noise was much higher than that of the prediction results. This error may stem from the fact that the boundary layer displacement thickness was not predicted well at low wind speeds due to a laminar–turbulent transition.

In addition, we removed the mechanical noise from the measured sound signal and compared the sound pressure levels of the numerical predictions and the experimental data. High-pass filter was applied to the measured sound signal. This filter had a cut-off frequency of 250 Hz, and its attenuation level in the stop band was over 20 dB. Fig. 5 compares the sound pressure levels of the high-pass filtered signal and the numerical predictions. At wind speeds between 3 m/s and 5 m/s, the level difference between the experimental data and the numerical predictions was up to about 5 dB. As already seen from Fig. 4, this error was due to the under-prediction of the trailing edge bluntness noise. However, at wind speeds over 5 m/s, the sound pressure level of the numerical predictions agreed with that of the filtered signals within 2 dB. This confirms that the under-prediction shown in Fig. 3 was partly because of the low frequency mechanical noise.

The measurement results indicate that the trailing edge bluntness noise is one of the dominant noise sources, although a previous study showed for a large wind turbine that the trailing edge bluntness noise is unimportant [8]. Trailing edge bluntness noise is generated provided that the height of the trailing edge is larger than about one-fifth of the boundary layer displacement thickness [8]. The trailing edge of the blade used in the experiment had a round shape and a diameter of about 4 mm at the tip. To compare the boundary layer displacement thickness and the trailing edge height for the blades, the boundary layer displacement thickness of the outboard region is predicted using the XFoil code [9]. Table 1 presents the calculated boundary layer displacement thickness at various wind speeds. In Table 1, the peak frequency represents the predicted peak frequency for the trailing edge bluntness noise, and the minimum trailing edge height is the estimated minimum trailing edge height at which the trailing edge bluntness noise occurs. The results show that the ratios between the trailing edge thickness and the boundary layer displacement thickness were

over 0.2 at all wind speeds; this led to the generation of the trailing edge bluntness noise.

In practice, it is difficult to make blades with a sharp trailing edge because wind turbine blades are typically made of fiber-reinforced plastic. For a typical wind turbine blade, the trailing edge thickness is about 1 mm–3 mm [5]. For large wind turbine blades, the boundary layer displacement thickness is much higher than this range of thickness. However, for small wind turbine blades, the trailing edge thickness should be less than 1 mm to avoid trailing edge bluntness noise. Therefore, the results of this study indicate that for a small wind turbine, trailing edge bluntness noise can easily occur unless the blades have very sharp trailing edges.

## 5. Conclusion

In the present study, the aerodynamic noise from a 10 kW wind turbine was predicted using semi-empirical models, and the prediction results were compared with field measurement data. The comparison results indicated that although trailing edge bluntness noise was under-predicted at low wind speeds, the spectral trends of the prediction results generally agreed well with those of the field experiment. It was also found for small wind turbines that trailing edge bluntness noise can be a dominant noise source unless the wind turbine blades have very sharp trailing edges. The numerical modeling procedure used in this study and the results of the noise measurements will be useful for the design of small wind turbines having low noise levels.

## Acknowledgments

This work was supported by the Human Resources Development program (No. 20124030200030) of the Korea Institute of Energy Technology Evaluation and Planning (KETEP) grant funded by the Korea Government Ministry of Trade, Industry and Energy. This research was also supported by the Institute of Advanced Aerospace Technology at Seoul National University.

## References

- [1] Zhu WJ, Heilskov N, Shen WZ, Sørensen JN. Modeling of aerodynamically generated noise from wind turbines. *J Sol Energy Eng* 2005;127:517–28.
- [2] Oerlemans S, Schepers JG. Prediction of wind turbine noise and validation against experiment. *Int J Aeroacoustics* 2009;8:555–84.
- [3] Lowson MV. Theory and experiment for wind turbine noise. AIAA Paper 94-0119. In: 32nd Aerospace sciences meeting and exhibit 1994.
- [4] Brooks TF, Pope DS, Marcolini MA. Airfoil self-noise and prediction. NASA reference publication 1218; 1989.
- [5] Wagner S, Bareiß R, Guidati G. Wind turbine noise. Berlin: Springer-Verlag; 1996.
- [6] Counihan J. Adiabatic atmospheric boundary layer: a reviewed and analysis of data from the period 1880–1972. *Atmos Environ* 1975;9:871–905.
- [7] IEC 61400-11. Wind turbine generator systems—part 11: acoustic noise measurement techniques. International Electrotechnical Commission; 2002.
- [8] Oerlemans S, Sijtsma P, Méndez López B. Location and quantification of noise sources on a wind turbine. *J Sound Vib* 2007;299:869–83.
- [9] <http://web.mit.edu/drela/Public/web/xfoil/> [accessed 13.06.2013].